

The influence of sea surface temperature for vertical extreme wind shear change and its relation to the atmospheric stability at coastal area

Geonhwa Ryu¹, Young-Gon Kim², Dongjin Kim³, Sang-Man Kim⁴, Min Je Kim⁵,
Wonbae Jeon⁶ and Chae-Joo Moon^{*7}

¹OWC, Republic of Korea

²Wind Energy Research Center, Energy Valley Industry-University Convergence Agency, Republic of Korea

³Division of Earth Environmental System, Pusan National University, Republic of Korea

⁴Smart Grid Institute, Mokpo National University, Republic of Korea

⁵Department of Electrical and Control Engineering, Mokpo National University, Republic of Korea

⁶Department of Atmospheric Sciences, Pusan National University, Republic of Korea

⁷Department of Electrical and Control Engineering, Mokpo National University, Republic of Korea

(Received February 18, 2022, Revised March 15, 2023, Accepted March 23, 2023)

Abstract. In this study, the effect of sea surface temperature (SST) on the distribution of vertical wind speed in the atmospheric boundary layer of coastal areas was analyzed. In general, coastal areas are known to be more susceptible to various meteorological factors than inland areas due to interannual changes in sea surface temperature. Therefore, the purpose of this study is to analyze the relationship between sea surface temperature (ERA5) and wind resource data based on the meteorological mast of Høvsøre, the test bed area of the onshore wind farm in the coastal area of Denmark. In addition, the possibility of coastal disasters caused by abnormal vertical wind shear due to changes in sea surface temperature was also analyzed.

According to the analysis of the correlation between the wind resource data at met mast and the sea surface temperature by ERA5, the wind speed from the sea and the vertical wind shear are stronger than from the inland, and are vulnerable to seasonal sea surface temperature fluctuations. In particular, the abnormal vertical wind shear, in which only the lower wind speed was strengthened and appeared in the form of a nose, mainly appeared in winter when the atmosphere was near-neutral or stable, and all occurred when the wind blows from the sea. This phenomenon usually occurred when there was a sudden change in sea surface temperature within a short period of time.

Keywords: atmospheric stability; Richardson number; sea surface temperature; wind shear warning; wind shear

1. Introduction

The inter-relationship between the atmosphere and the ocean causes changes in their characteristics and influences both local meteorological events in the short term and long-term climate change. Among them, changes in sea surface temperature (SST) affect the heat flux exchange of water vapor, causing changes in the atmospheric boundary layer (ABL) in the ocean and coastal areas (Liu *et al.* 2007). In particular, an increase in the SST in summer causes the convergence of water vapor in the lower atmospheric boundary layer, causing the atmospheric stability to be unstable, potentially changing meteorological phenomenon and local climate in coastal areas. In this regard, Fan *et al.* (2016) reported that sea surface temperature anomalies in tropical seas can influence the Asian monsoon in summer and determine the shape of precipitation. Qu *et al.* (2012) found that the North Atlantic Oscillation (NAO) has a significant correlation with sea surface temperature, wind, and sea ice area surrounding Greenland.

Depending on the climatic characteristics, the

interaction between the atmosphere and the ocean can be more active in coastal areas than inland, resulting in rapid changes in the fluidity of the atmosphere in the atmospheric boundary layer in coastal areas in a short period of time (Cui *et al.* 2021, Andrea *et al.* 2021). In particular, compared to inland areas where the amount of water vapor in the atmosphere is relatively small, frequent fogging due to a large inflow of water vapor, typhoon damage due to a continuous supply of latent heat, or large amounts of precipitation all year due to wind and flood damages will limit daily human life in coastal and offshore areas. Above all, the active interaction of the ocean with the atmosphere implies that it is susceptible to direct and indirect wind damage, which is directly related to the flow characteristics of the atmosphere (Ryu *et al.* 2021).

In the case of complex mountainous terrain, hilly or coastal areas, strong low-level vertical wind shear may occur in the vertical direction due to the large wind speed difference between the upper and lower layers under the atmospheric boundary layer (Chae *et al.* 2020). In general, wind shear occurs near the upper jet stream or near the tropospheric interface altitude, but it often occurs when a strong downdraft is accompanied by a strong wind speed in the upper layer or the front where air masses meet in the lower atmosphere.

Wind shear can quickly diffuse floating air pollutants

*Corresponding author, Ph.D. Professor
E-mail: cjmoon@mokpo.ac.kr

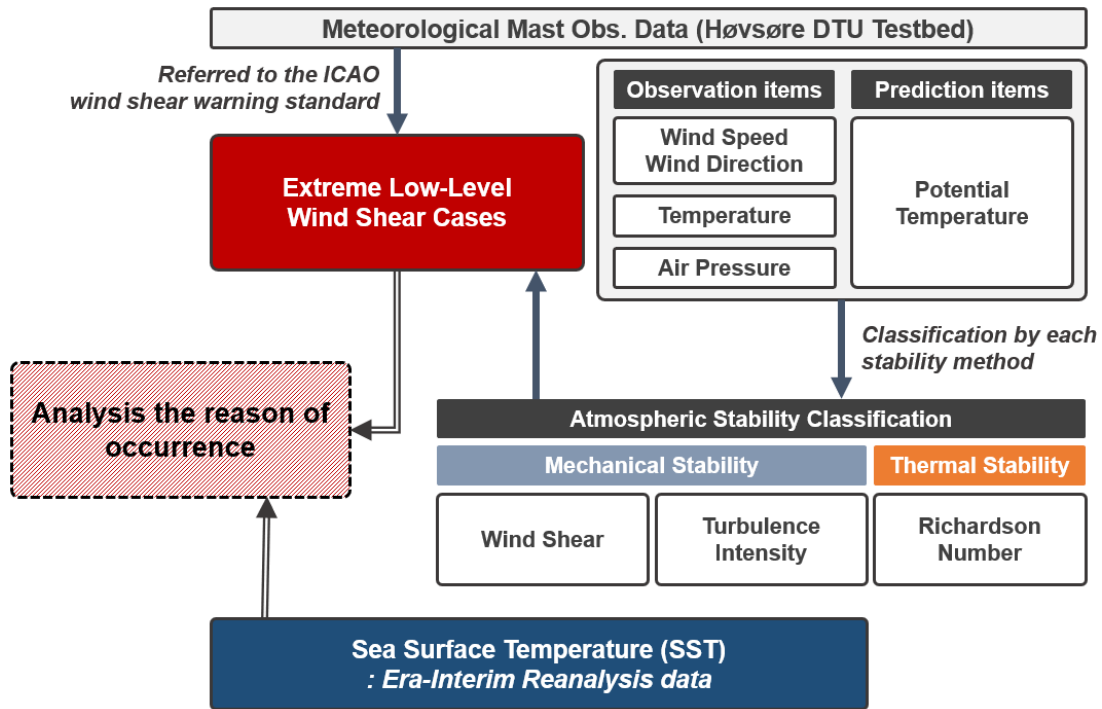


Fig. 1 Introduction to research procedures and methodologies

and dilute their concentration in the atmosphere, but in some cases, it can cause physical damage, such as the appearance of strong meteorological disasters and building collapses (Piotr *et al.* 2021, Huang *et al.* 2021).

Ashok (2002) reported that the concentration of pollutants in the atmosphere can be rapidly diluted when vertical wind shear is active in coastal areas. However, Klotz and Jiang (2017) mentioned that the movement and strength of tropical cyclones can be determined by the direction and magnitude of wind shear. Wen *et al.* (2017) also revealed that the power output by the wind turbines decreased as the vertical wind shear became stronger, and the load was transmitted strongly to the blades, which could shorten the life of the turbine. Hunter *et al.* (2001) also reported that the amount of wind power generation was decreased by more than 40% when a strong vertical wind shear occurred.

Golding (2005) stated that the vertical wind shear at a low level near the surface greatly impedes the take-off and landing of aircraft, and is regarded as one of the major causes of aviation accidents worldwide every year. According to Dennis and Kumjian (2017), as the wind shear magnitude increased, the updraft of the storm became stronger, the amount and mass of hail increased, and the residence time in the atmosphere became longer. Shen *et al.* (2013) reported that vertical wind shear develops a thick atmospheric mixing layer, which disturbs the rainfall system in southern China in early summer and contributes to large-scale heavy rainfall.

Similarly, vertical wind shear, which can readily occur near coastal areas, can produce significant disasters and large-scale damage depending on the exact environmental situation (Ryu *et al.* 2022a, 2022b). It is well documented that the creation and dispersion of turbulence is influenced

by the sea surface temperature, which dictates the amount of vertical wind shear, that can last for a few hours or several months (Yoo *et al.* 2014). It is reported that the cold water zone generated in coastal areas is closely related to land-sea breeze circulation and wind speed change (Ji *et al.* 2014). The magnitude of this vertical wind shear can be influenced by local atmospheric stability changes. When constructing an offshore wind farm, it is recommended to construct wind turbines in an area with relatively little change in atmospheric stability by analyzing the atmospheric stability of various sites in advance. In addition, more efficient wind farm operation may be possible if the wind turbine design load is higher than that of other regions in areas with strong vertical wind shear (Kim *et al.* 2021b).

In particular, prior to the development of offshore wind farms, which are rapidly progressing along with the carbon neutrality issue, it is necessary to conduct prior research on the regional climate or micro-meteorological characteristics of wind resources in coastal areas.

Therefore, in this study, the purpose of this study was to investigate the effect of coastal sea surface temperature changes on atmospheric stability and vertical wind shear using a meteorological mast operated in a test bed for a wind farm in Høvsøre, a coastal area in Denmark. The analysis procedure is shown in Fig. 1, and the process is as follows.

- After conducting a basic wind resource characteristic analysis using the meteorological mast observation data, low-level wind shear reinforcement cases that correspond the ICAO wind shear warning standards are extracted.
- Through atmospheric stability analysis, classify when the atmospheric conditions are the main occurrence of such abnormal phenomena.

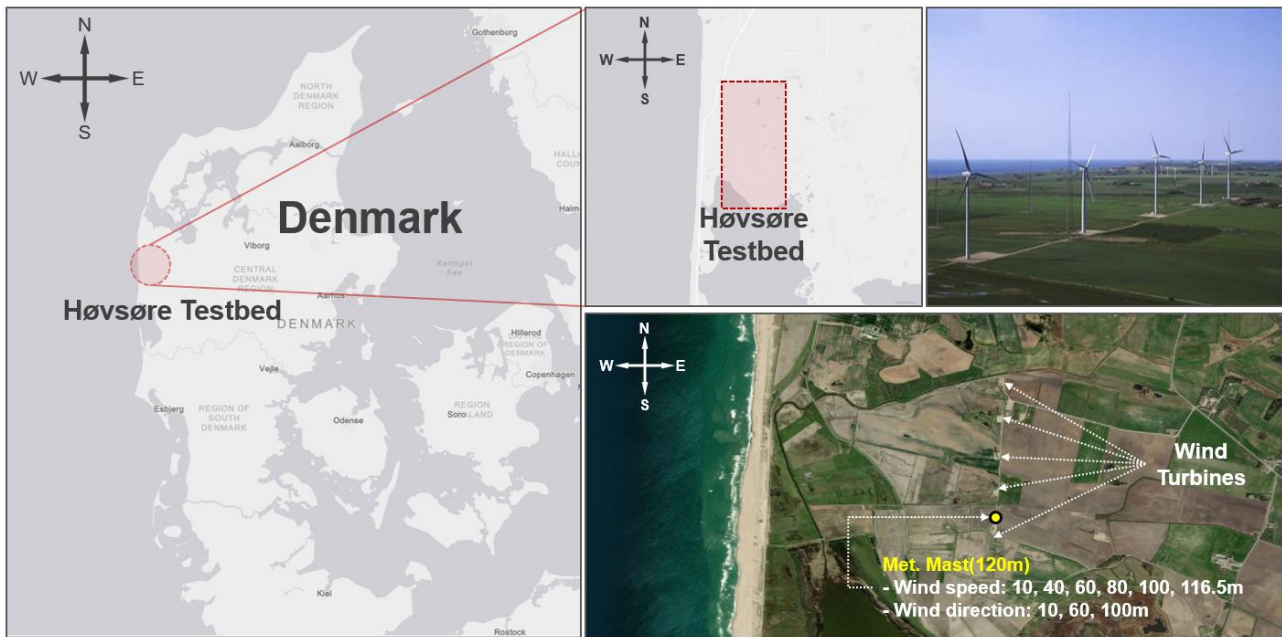


Fig. 2 Satellite view of DTU Høvsøre testbed and meteorological mast in Denmark coastal site

Table 1 Meteorological mast observation data and reanalysis data information

Site		Høvsøre DTU test site (56.44°N, 8.14°E)	
Data period		2014.01.01. ~ 2014.12.31. (1hr averaged)	
		Mast height[m]	120
		Data	Wind speed(WS), Wind direction(WD), Air temperature(T), Air pressure(P)
Met. mast		WS	10, 40, 60, 80, 100, 116.5
		WD	10, 60, 100
Analysis Data	Measurement height [m]	T	2, 100
		P	2, 100
	Name	Era-interim	
	Producer	ECMWF	
	Resolution	0.75°×0.75°	
Reanalysis data		Sea surface temperature (SST)	
	Data	Surface Sensible heat flux (SSHF)	
		Vertical Velocity (VV)	

• Analyze whether the case of low-level wind shear reinforcement in the coast is closely related to the change in sea surface temperature within a short time.

This is to promote structural stability of offshore wind turbines and to understand changes in coastal meteorological characteristics due to local climate change.

2. Data and methods

2.1 Site and meteorological data

The target area includes the wind farm test bed operated

by the wind energy research institute of DTU (Denmark Technical University) in Denmark. The provided wind speed data were 10, 40, 60, 80, 100, and 116.5 m, and the atmospheric parameters (air pressure, air temperature) were analyzed in units of one hour from January 1 to December 31, 2014 (Pedersen *et al.*, 2019). There were total of 7 megawatt-scale onshore/offshore wind turbine test areas in the test bed site, and the purpose was to acquire certification for turbine safety, power performance, and noise emission.

As shown in Fig. 2, the target site was located about 1.7 km from the west coast of Denmark. The surrounding terrain was flat with an elevation of 3 m above sea level and consisted of wide grassland. A total of five wind turbines

Table 2 Atmospheric stability indices criteria and atmospheric boundary layer properties.

	Wind shear exponent	Richardson number	ABL* properties
Strongly Unstable	$\alpha < 0.0$	$R_f < -0.86$	Lowest wind speed and shear, Highly TI*
Unstable	$0.0 \leq \alpha < 0.1$	$-0.86 \leq R_f < -0.1$	Lower wind speed and shear, High TI
Near-Neutral	$0.1 \leq \alpha < 0.2$	$-0.1 \leq R_f < 0.053$	Logarithmic wind profile
Stable	$0.2 \leq \alpha < 0.3$	$0.053 \leq R_f < 0.134$	High wind speed and shear, Low TI
Strongly Stable	$\alpha \geq 0.3$	$R_f \geq 0.134$	Highest wind speed and shear, Lowest TI

*ABL: Atmospheric boundary layer

*TI: Turbulence intensity

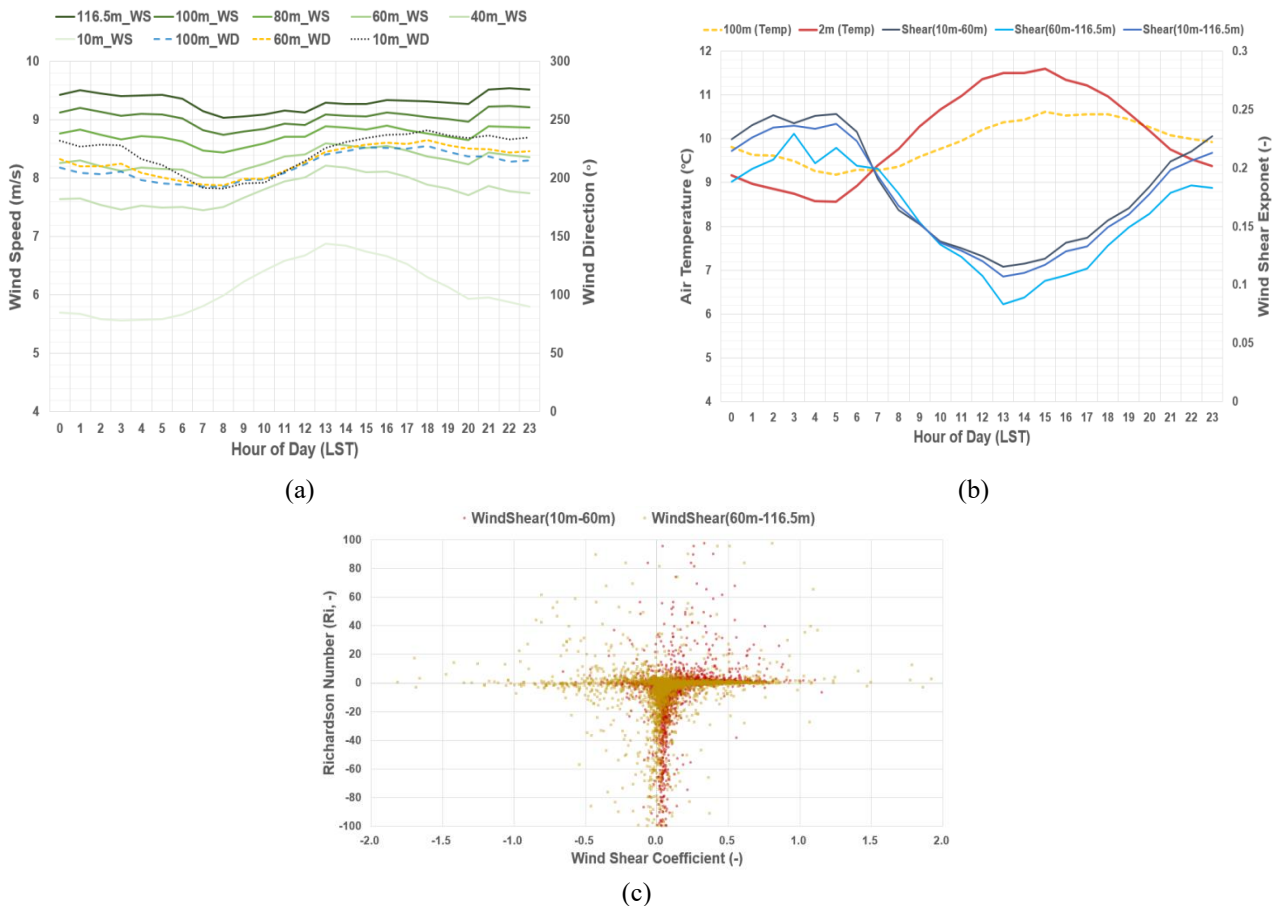


Fig. 3 Time series graphs using meteorological observation data. (a) Diurnal change of wind speed and wind direction; (b) diurnal change of vertical wind shear and air temperature; (c) scatter plot between vertical wind shear and Richardson number (Red circles-wind shear at 10-60 m, yellow squares-wind shear at 60-116.5 m)

were located in the north-south direction, and a 120 m high meteorological mast (56.44°N, 8.14°E). Since March 1, 2004, the DTU wind research institute has been measuring wind speed, wind direction, air temperature and pressure, and relative humidity. This testbed is located on the coast, but is actually a site to test offshore wind turbines. This is because during testing, technicians always have direct access to the wind turbine when they need to change components and maintain the turbine. Offshore, it is impractical to test a prototype wind turbine because of the many restrictions on turbine operation.

Sea surface temperature was extracted from the reanalysis data of Era-interim (ECMWF ReAnalysis

Interim) (Dee *et al.* 2011) provided by the European Center for Medium-Range Weather Forecasts (ECMWF). The data period was same as the observation data, i.e., from January 1 to December 31, 2014, and the resolution was $0.75^\circ \times 0.75^\circ$, which corresponded to about 80 km in mid-latitude.

2.2 Atmospheric stability

Atmospheric stability is an important factor used to define atmospheric turbulence or to describe the magnitude of atmospheric diffusion (Kim *et al.* 2021a). It refers to the degree to which the atmosphere in a state of mechanical equilibrium is slightly disturbed to return to its original state

or the state of the atmosphere is likely to change significantly. Atmospheric stability can be classified into three stages: unstable, neutral, and stable. Atmospheric stability can be broadly classified as mechanical stability and thermal stability. Atmospheric stability based on Richardson number including changes in temperature or heat flux is called “thermal atmospheric stability”, and atmospheric stability based on wind shear and turbulence intensity without thermal factors can be called “mechanical atmospheric stability”.

Table 2 shows the stability criteria of wind shear, which is a representative mechanical atmospheric stability index, Richardson number, which means thermal atmospheric stability, and atmospheric boundary layer characteristics (Wharton and Lundquist 2012).

2.2.1 Wind shear exponent

The wind shear exponent in power law represents a mechanical atmospheric stability. When the atmospheric stability is near-neutral state, the vertical wind speed distribution in which the wind speed constantly increases according to the height (Ryu *et al.* 2016). The wind shear exponent (α) is a correction factor that follows the ground state around the observation point as shown in Eqs. (1)-(2). The power law exponent is therefore the gradient of a line fit by the least squares method to the log of the wind speed, and the log of the height. The exponent is not constrained as a wide range of wind shear can occur under non-neutral conditions (Wagner *et al.* 2009).

$$\frac{U}{U_r} = \left(\frac{Z}{Z_r}\right)^\alpha \quad (1)$$

$$\alpha = \frac{\ln(U) - \ln(U_r)}{\ln(Z) - \ln(Z_r)} \quad (2)$$

* r : reference height

2.2.2 Richardson number

The Richardson number is both an indicator of turbulence and stability. A very negative Richardson number indicates that convection prevails and winds are weak with a strong vertical motion characteristic of an unstable atmosphere. As the mechanical turbulence increases, the Richardson number approaches zero with a neutral stability ($\partial\theta/\partial z = 0$). Finally, as the Richardson number increases, vertical mixing stops and the atmosphere begins to stratify, resulting in mechanical turbulence (Lu *et al.* 2020).

$$S = \frac{g}{T} \left(\frac{\Delta\theta}{\Delta Z}\right) \quad (3)$$

$$\theta = T \left(\frac{p_0}{p}\right)^{0.286} \quad (4)$$

$$Ri = \frac{S}{(\partial\bar{u}/\partial Z)^2} = \frac{g}{T} \frac{(\partial\theta/\partial Z)}{(\partial\bar{u}/\partial Z)^2} = \frac{g}{T_0} \frac{(\partial/\partial Z)[\theta_0 + \theta_1]}{[(\partial/\partial Z)(u_0 + u_1)]^2} \quad (5)$$

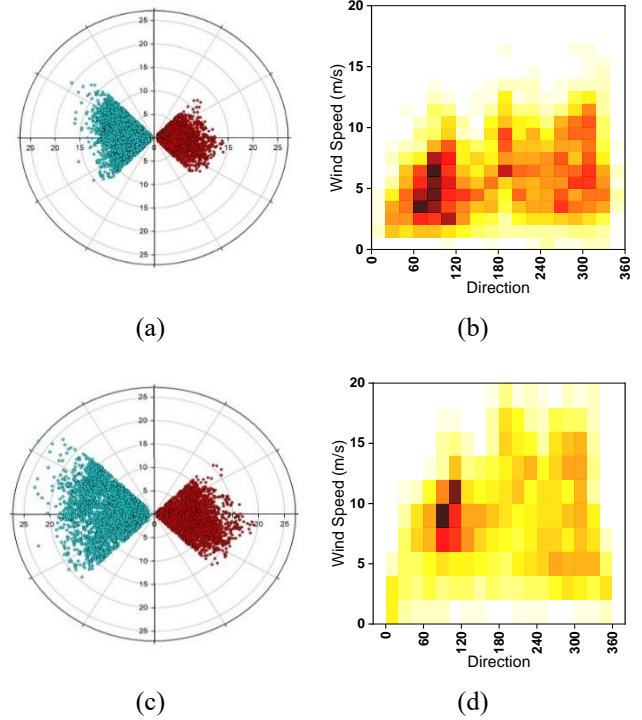


Fig. 4 Wind speed scatter plots and heatmaps according to the wind direction. (a)-(b) 10 m; (c)-(d) 100 m. Blue dots and red dots represent wind speed from the sea and land, respectively.

3. Result analysis

3.1 Meteorological mast observation data

When the diurnal change of wind speed was examined at 6 heights of the meteorological observation tower, the wind speed at 10 m, which was the lowest layer, showed the highest wind speed at 1300 LST (Local Standard Time) (Fig. 3(a)).

However, the diurnal change pattern of the upper layer was different from that of the surface layer. This was because the surface heat flux that increased during the day formed a strong turbulence and increased the wind speed at near the surface. However, as the height was increasing, the heat flux emitted from the surface did not reach the upper layer, therefore the increase in wind speed remained unaffected.

As a result, the difference in wind speed between the upper and lower layers became smaller during daytime and larger at nighttime. In other words, the generation and strength of turbulence in the vertical direction are affected by the temperature gradient between the upper and lower layers, which has an impact on vertical wind shear production and disappearance. As shown in Fig. 3(b), during the day when the temperature of the upper layer (100 m) was lower than that of the lower layer (2 m), the vertical convection became active and the difference in wind speed by height became smaller.

The Richardson number was calculated using the wind speed, air temperature, and potential temperature data at the

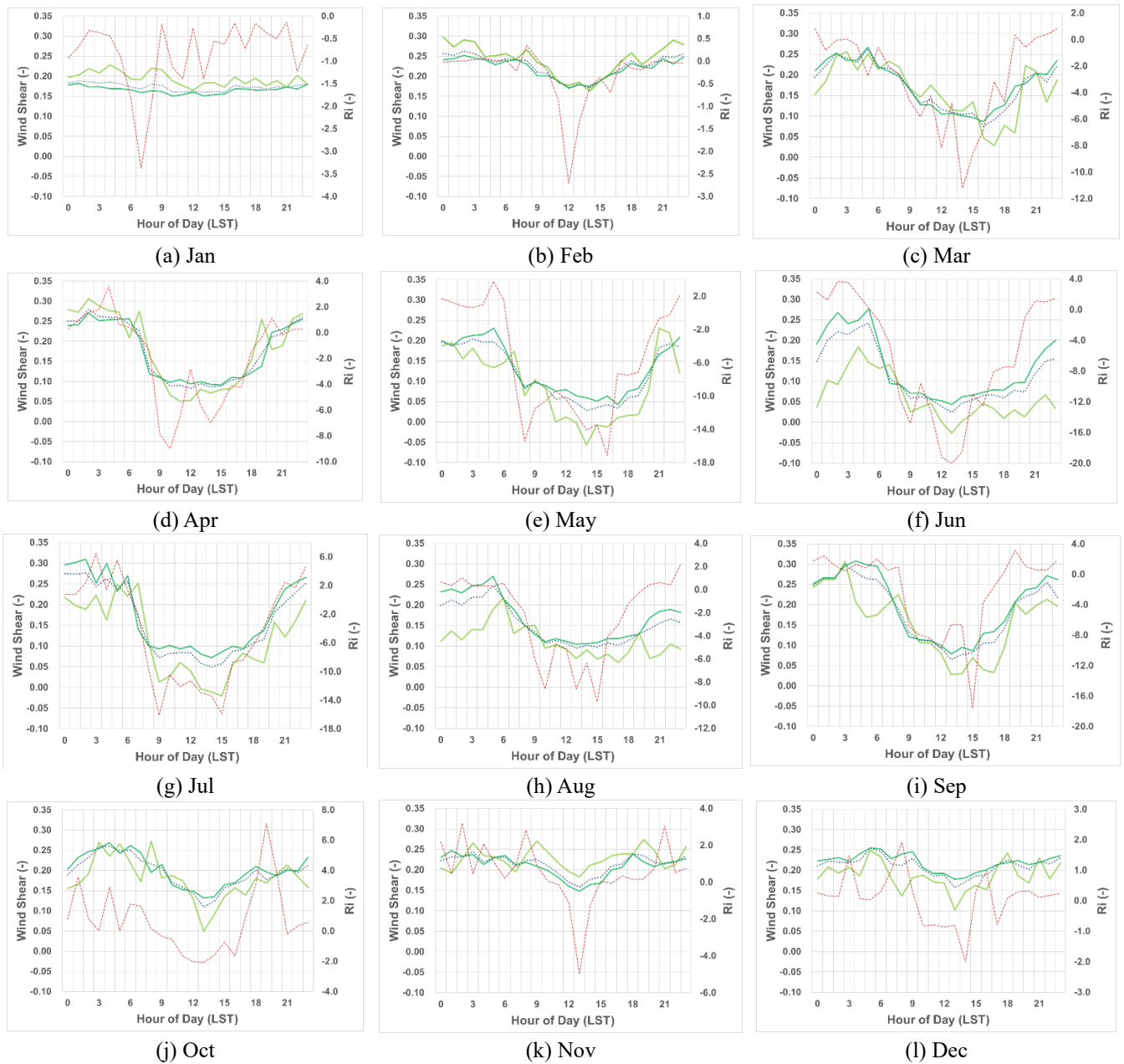


Fig. 5 Monthly diurnal wind shear and Richardson number change. Red dashed line: Richardson number; Green solid line: wind shear at 10 m and 60 m; Light green solid line: wind shear at 60 m and 116.5 m; Blue dotted line: wind shear at 10 m and 116.5 m

heights of 10 m and 100 m. From now on, the wind shear between 10 m and 60 m is referred as the low-level wind shear (LLWS) and the wind shear between 60 m and 116.5 m is referred as the upper level wind shear (ULWS). As shown in Fig. 3(c), the LLWS showed a relatively positive value, however, since it was directly affected by the heat flux of the land surface, it was more unstable than the ULWS in terms of thermal atmospheric stability.

In order to investigate the wind speed variation characteristics of wind resources blowing from the sea and land, the observed wind speed of each direction is shown in Fig. 3. In the case of the north ($0^\circ \pm 45^\circ$) and south ($180^\circ \pm 45^\circ$) sector, where the wind turbines and meteorological towers were installed, the wind data may be

distorted by the wake effect of the turbine. For that reason, only the direction from the sea (225° to 315°) and the direction from the land (45° to 135°) were analyzed. As a result of the analysis of the 10 m wind, the average wind speed from the sea was 6.86 m/s, while that from the land was 5.12 m/s (Figs. 4(a) and 4(b)). The wind showed the same pattern at a height of 100 m. The average wind speed from the sea reached 9.88 m/s and the average wind speed from the land was 8.12 m/s (Figs. 4(c) and 4(d)). Regardless of the height, the wind speed from land showed a lower value than that of the sea because the highly friction caused by the large surface roughness of the land affected the wind.

Fig. 5 shows the monthly diurnal change of the wind shear coefficient and Richardson number using

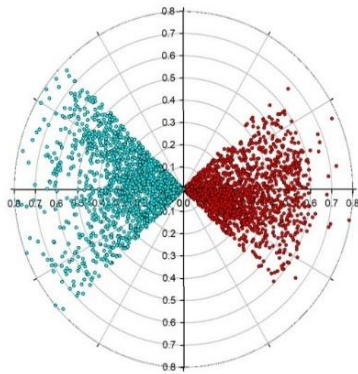


Fig. 6 Vertical wind shear coefficients (10 m-116.5 m) scatter plots according to the wind direction. Blue dots: from sea, Red dots: from land

meteorological mast observed data by height. In general, the wind shear coefficient was used as an indicator of atmospheric stability excluding thermal factors, and represented the rate of increasing/decreasing vertical wind speed gradient. The vertical distribution of wind speed through the power law can be applied only in the lower part of the atmospheric boundary layer where the change of wind speed according to height was uniform (Wagner *et al.* 2009).

Wind speeds of 10 m and 60 m, 60 m and 116.5 m, and 10 m and 116.5 m, respectively, were used to confirm the monthly averaged change of vertical wind shear coefficient. Overall, the wind shear coefficient showed continuous high value and small change trend in winter, forming a neutral and stable atmospheric condition. In contrast, in summer season, the wind shear coefficient was below 0.1 in daytime, indicating that the atmosphere was unstable. This was because there was no significant difference in wind speed by height due to active atmospheric vertical mixing from the heated surface layer.

The same result was derived from the change pattern of the Richardson number, which indicated thermal atmospheric stability. In winter, except for noon, most of the near-neutral or stable state was dominant, while in the summer, it showed a strong negative indicator and extremely unstable atmospheric conditions continued throughout the day.

Fig. 6 shows the vertical wind shear coefficients using wind speed at 10 m and 116.5 m blowing from the sea and land, respectively. As confirmed in Fig. 3, in the case of the wind blowing from the sea, the wind speed of the upper layer is strong, so the averaged wind shear coefficient was 0.283, showing a relatively large difference compared to the opposite case (from land), which showed 0.166.

3.2 Era-Interim reanalysis data

Because the wind shear coefficient of wind blowing from the sea was higher than that of wind blowing from the land, it was found that not only the roughness of the ground, but also the air pressure and air temperature arrangement of the sea and land were important. The monthly averaged changes in sea surface temperature and offshore wind speed

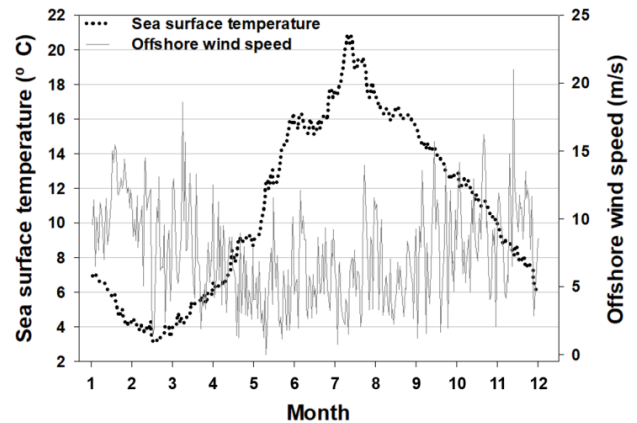


Fig. 7 Daily mean sea surface temperature and offshore wind speed (10 m) near Høvsøre observation site using Era-Interim reanalysis data

Table 3 Wind shear warning standard manual

Intensity	Variation of wind
Light	0-4 knots per 100 feet
Moderate	5-8 knots per 100 feet
Strong	9-12 knots per 100feet
Severe	Above 12 knots per 100 feet

near the Høvsøre meteorological mast using Era-Interim data are shown in Fig. 7. In the case of sea surface temperature, it exceeded 20°C between July and August, and the lowest value was recorded between February and March. In the case of offshore wind speed (10 m height), the overall wind speed value was higher than that of land, and the pattern showing the lowest wind speed in summer and the highest wind speed in winter was the same. It is noteworthy that the pattern of change in sea surface temperature and offshore wind speed was reversed, as evidenced by the fact that the sea surface temperature was highest in summer and the offshore wind speed was lowest in winter.

It is analyzed the vertical velocity and sensible heat flux (Era-interim) data at sea 11 km northwest of the meteorological mast (Fig. 8). The sensible heat flux showed a general pattern of increasing from 0900 LST throughout the year, and decreased again at 1700 or 1800 LST. A high sensible heat flux indicates that solar radiation is dominant, and in this case, the vertical velocity increases according to the vertical convection because the surface is heated. In some graphs, it may seem that the vertical velocity and the sensible heat flux are inversely proportional. It is because the time when the vertical velocity starts to increase and the time when the sensible heat flux increases due to the specific heat of the sea are shifted by several hours.

3.3 Risk analysis by the wind shear coefficient

In general, according to the International Civil Aviation Organization (ICAO), vertical and horizontal wind shear is defined as a case in which the wind speed and direction change rapidly, and warning standards according to the

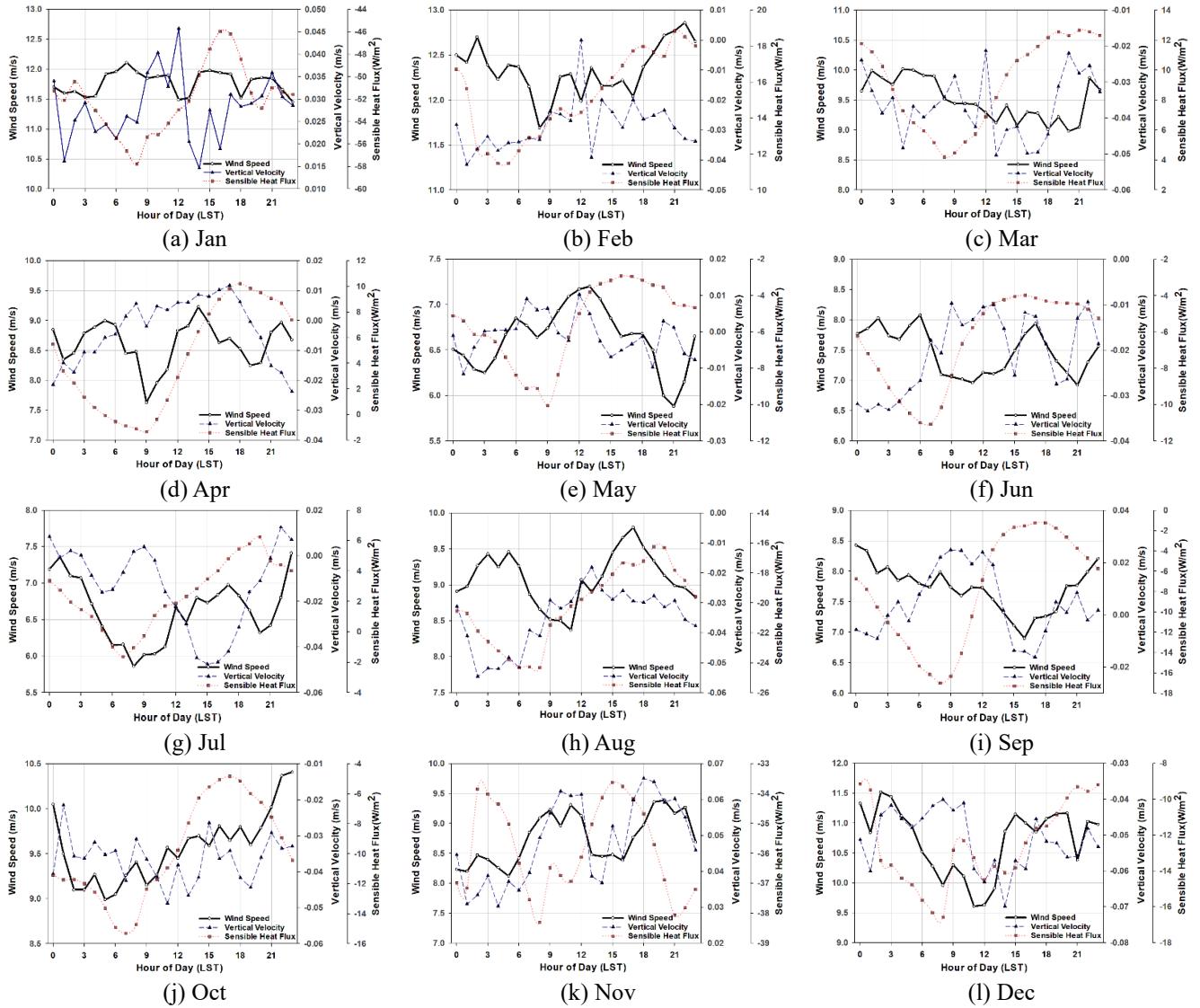


Fig. 8 Monthly diurnal wind speed, vertical velocity and sensible heat flux. Black Solid line: Wind speed at 100 m; Red dotted line: Sensible heat flux at 2 m; Blue dashed line: Vertical velocity at 100 m

strength of the wind shear is suggested (Table 3). The level of wind shear warning is defined according to the change in wind speed by height for every 100 feet, and the most serious level is when the wind speed changes exceed 12 knots (about 6.2 m/s) for ascending or descending 100 feet (about 30 m). If a sudden strong wind shear is encountered near the ground, the aircraft may experience a shock that causes it to strain as it approaches the runway. The ICAO regulations were examined to determine how large a wind shear must be to be classified as dangerous to structures, such as wind turbines.

Cases suitable for issuing warning standards were classified by applying the observation wind speed change by height of the meteorological mast in the same way as the ICAO warning standards. Accordingly, cases in which the difference between the wind speed at 10 m and 60 m heights, which corresponded to the normal living height of humans, exceeding 5 m/s, were selected. And then the averaged wind shear coefficient at that time was also calculated. Likewise, in the case where the wind speed

difference between 60 m and 100 m did not exceed 2.0 m/s was selected. This was to select cases in which the wind shear of the lower layer was strong but the wind shear of the upper layer was relatively weak.

As shown in Table 4, the cases satisfying the warning criteria lasted for 54 hours over the course of the year in 2014, mostly in the winter, and the typical wind shear coefficient was around 0.2 at the time. Most of the cases in which the wind speed near 60 m was abnormally strong within a height of 100 m occurred in winter. At this time, the atmospheric stability analysis result using the Richardson number indicated that the atmosphere was in a stable or near-neutral state.

After examining the wind direction distribution to determine in which environment the selected cases primarily occur, it was discovered that they all match circumstances where the wind blows from the sea (Fig. 11). The wind blowing from the offshore without large obstacles showed a large wind shear scale in the vertical direction in the lower layer, and the author tried to analyze the cause by

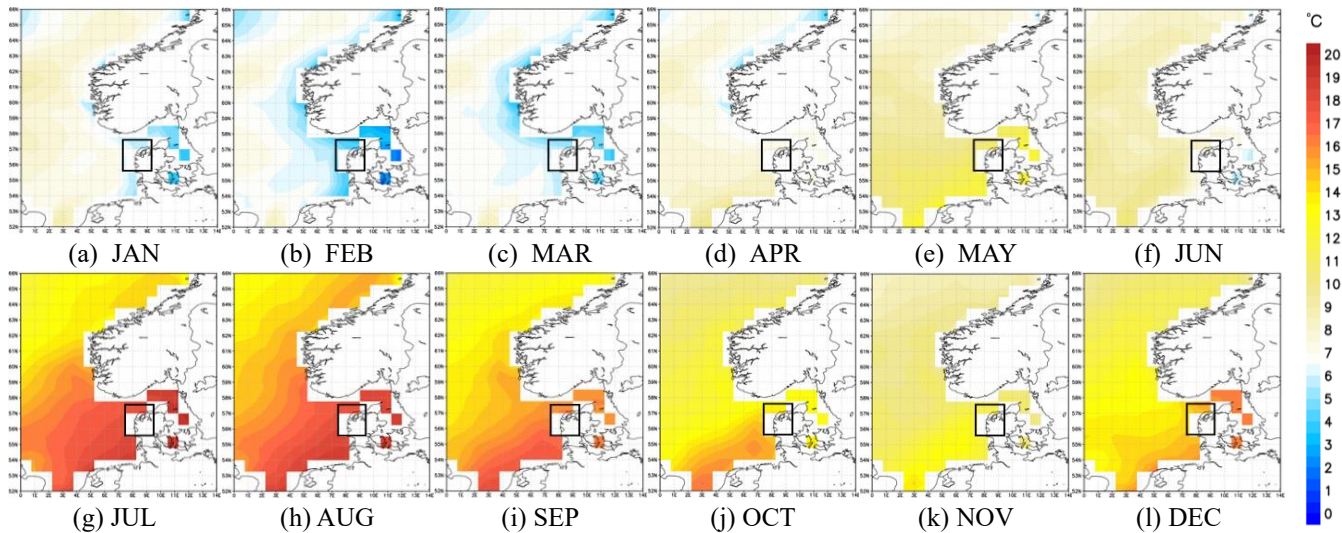


Fig. 9 Monthly averaged sea surface temperature distribution over North Sea using ERA-Interim reanalysis data. Black square includes the study domain.

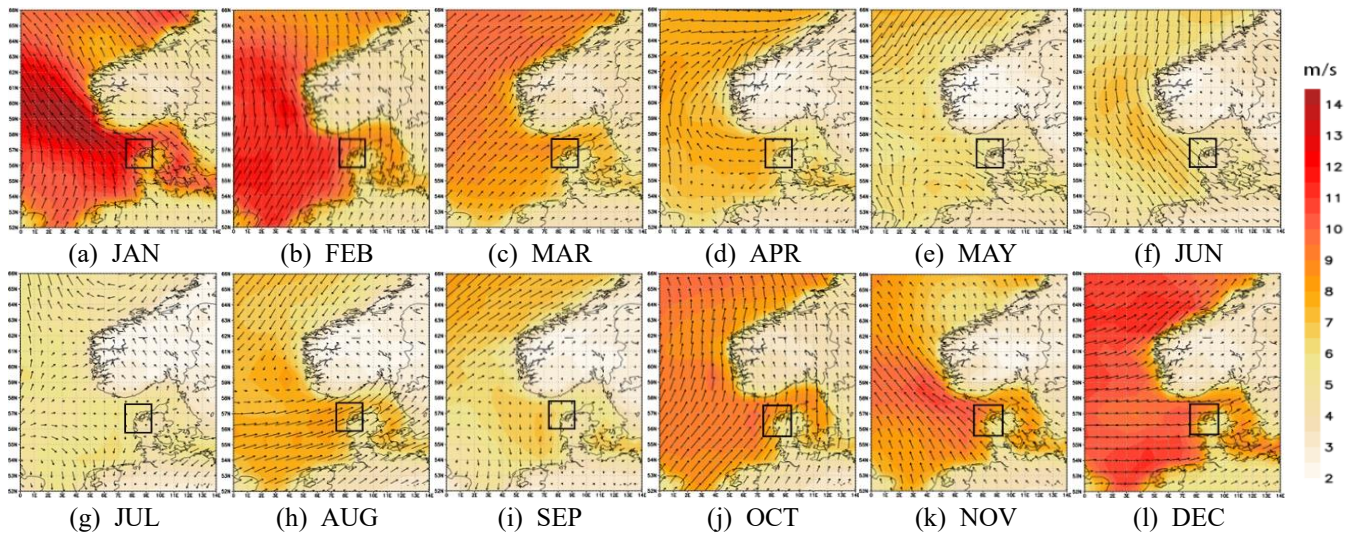


Fig. 10 Monthly averaged offshore wind speed distribution and wind vectors over North Sea using ERA-Interim reanalysis data. Black square includes the study domain.

Table 4 Case of wind shear warning in Høvsøre

Item	Properties			
Criteria	Above 5 m/s gap between 10 m and 60 m, and then below 2.0 m/s gap between 60 m and 100 m			
Number of cases	54 hours (out of 8741 hr)			
Season	spring	1.85%	summer	3.70%
	autumn	0%	Winter	94.45%
Averaged wind shear coefficient	10 m-60 m		60 m-100 m	
		0.223		0.206
Atmospheric stability (Richardson number)	Strongly unstable			0%
	Unstable			5.56%
	Near-neutral			64.81%
	Stable			25.93%
	Strongly stable			3.70%

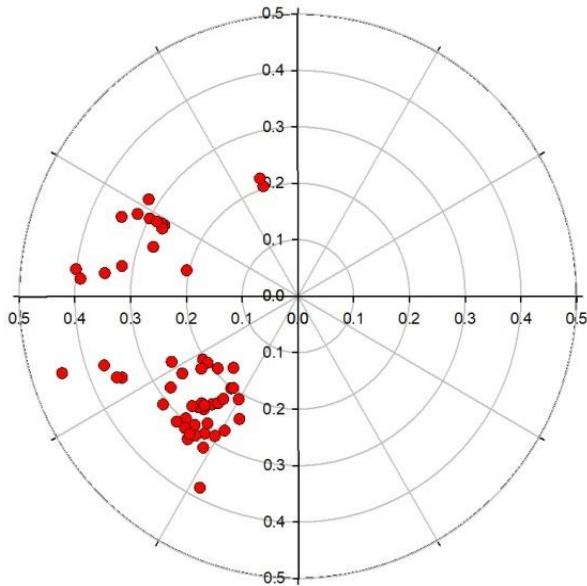


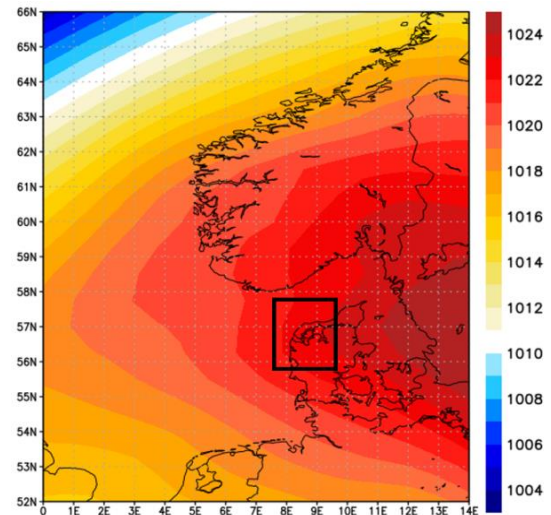
Fig. 11 Wind shear coefficient scatter plot of wind shear warning cases using meteorological mast data

judging that this phenomenon is related to the local characteristics of the offshore area.

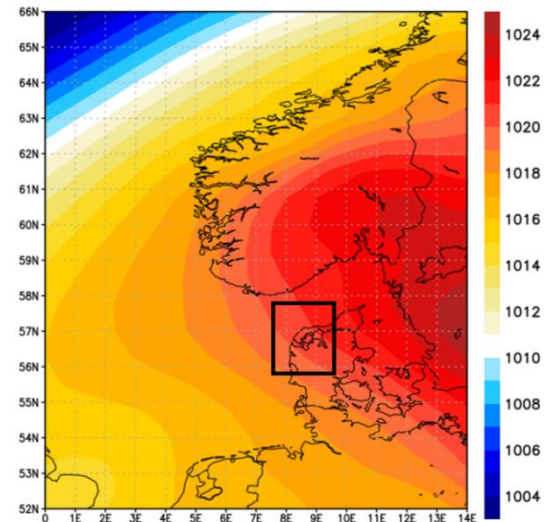
3.4 Case study of changes in wind shear coefficient due to sea surface temperature

Since the cases that cause strong wind shear were limited to wind direction blowing from the sea, cases were selected where the wind speed difference by height increased unexpectedly and analysed the sea level air pressure arrangement and sea surface temperature change at the time. On December 3, 2014, the wind speed difference between 10 m and 60 m was only 1.2 m/s, but 12 hours later, it increased to 4.5 m/s in 18 UTC and 5.3 m/s in 24 UTC, showing a significant change over a short period of time. When comparing the air pressure arrangement in the sea near the observation point to before the occurrence of strong wind shear (Fig. 12(b)), there was a tendency for the air pressure to decrease slightly (Fig. 12(a)). However, there was no significant change in the overall air pressure arrangement. The change in the sea surface temperature distribution was analysed to evaluate the contribution of the sea surface temperature change to the formation of strong wind shear, as it was judged that the effect of the change in atmospheric pressure was insignificant (Fig. 13). The sea level temperature in the area indicated by the blue square had a high distribution form above 11°C before substantial wind shear occurred, as shown in Fig. 13(a). On the other hand, when strong wind speed shear occurred, in the case of Fig. 13(b), the sea surface temperature in the area around the observation point decreased by 1.25°C on average. The general sea surface temperature difference according to the average 6-hour interval from 06 UTC to 00 UTC the next day in December 2014 was shown as the solid black line in Fig. 14.

However, the difference in sea surface temperature according to the time of the day when strong low-level wind shear occurred was larger than the average. As the sea



(a)



(b)

Fig. 12 Mean sea level pressure distribution according to (a) cases of weak vertical wind shear and (b) strong vertical wind shear event. Black square includes the observation site (unit : hpa).

surface temperature increased, the upper and lower wind speeds became similar due to the active vertical mixing of the atmosphere near the sea surface, and a weak mechanical wind shear was formed.

However, as the sea surface temperature decreased at night, the mixing action in the vertical direction within the boundary layer was weakened, and the wind speed for each height were clearly divided, and it was believed that the strong vertical wind shear was formed due to the strong wind speed of the upper layer and the lower wind speed of the lower layer. Also, as confirmed earlier, the concentration of strong wind shear cases in winter was also presumed to be due to the weakening of the vertical convection due to low sea surface temperature.

This indicated that the role of SST/winds on coastal circulation and climate formation cannot be neglected, even in a region where the coastal topography was complex and left strong imprint of coastal winds (Boe *et al.* 2011, Seroka *et al.* 2018).

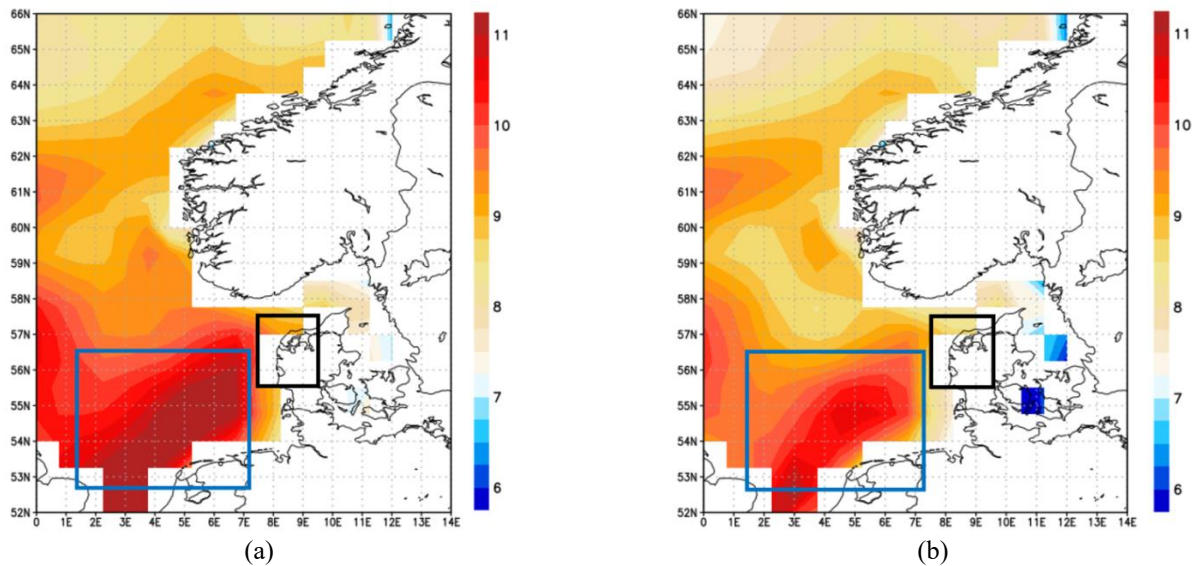


Fig. 13 Sea surface temperature distribution according to cases of weak vertical wind shear (a) and strong vertical wind shear event (b). Black square includes the observation site (unit : °C).

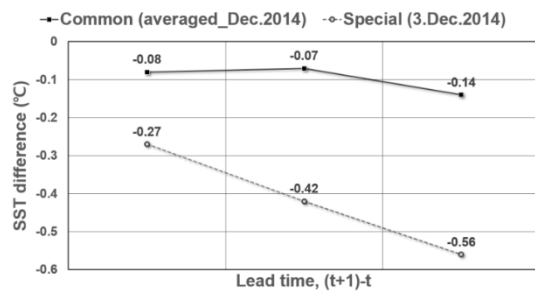


Fig. 14 sea surface temperature difference according to the average 6-hour interval from 06 UTC in December 2014 to 00 UTC the next day

4. Conclusions

In this study, the observation (wind resource) data of the meteorological mast located at the Høvsøre testbed in the coastal area of Denmark, and the sea surface temperature distribution of the Era-Interim reanalysis data was used to analyze the case where low-level strong wind shear occurred. The results of the three studies are summarized below.

1) As a result of analyzing observation data by height, there was no significant difference in wind speed by height during the daytime and summer when the heat flux exchange between the land surface and the atmosphere was active. On the other hand, as the vertical mixing action weakened at night and in the winter, the difference in wind speed according to height increased, resulting in the creation of an environmental characteristics where strong wind speed shear could easily occur.

2) Cases of strong wind shear were selected by similarly applying the wind shear warning criteria of the International Civil Aviation Organization (ICAO), and a total of 54 cases occurred throughout the year. At this time, the average wind shear coefficient was about 0.2, and 94% of the total selected cases were confined to winter.

A specific day was selected among the cases where very strong wind shear occurred, and as a result of using the Era-Interim reanalysis data to check the distribution of air pressure and sea surface temperature that has the most influence on the wind speed and direction in the coastal area.

Although there was no significant change in the atmospheric pressure distribution over time, it was confirmed that there was a large change in the sea surface temperature distribution.

3) Before the occurrence of strong vertical wind shear, the sea surface temperature was relatively high, and this caused a strong vertical mixing action along the coastal sites, which made the difference between the upper and lower wind speeds smaller. On the other hand, during the time of strong wind shear, the sea surface temperature decreased.

As a result of the separation between the upper layer's high wind speed and the lower layer's low wind speed, significant wind shear could occur. Due to the interaction between the atmosphere and the sea, which occurs actively in coastal areas, meteorological factors in the atmosphere and marine boundary layer can change rapidly, and accordingly, they can be easily exposed to damage for offshore/coastal wind turbines, such as the appearance of local severe weather phenomena, local climate change, and storms. In order to prevent and minimize damage by disasters such as strong wind speed shear and turbulence in coastal areas analyzed in this study, it is believed that evaluation such as the timing of occurrence and systematic climate factor analysis through various natural disasters damage cases is necessary.

Acknowledgments

This research was supported by "Regional Innovation Strategy (RIS)" through the National Research Foundation

of Korea (NRF) funded by the Ministry of Education (MOE)(2021RIS-002).

References

- Ashok, K.L. (2002), "The influence of vertical wind direction shear on dispersion in the convective boundary layer, and its incorporation in coastal fumigation models", *Bound. Layer Meteorol.*, **102**(1), 1-38. <https://doi.org/10.1023/A:1012710118900>.
- Boé, J., Hall, A., Colas, F., McWilliams, J.C., Qu, X., Kurian, J. and Kapnick, S.B. (2011), "What shapes mesoscale wind anomalies in coastal upwelling zones?", *Climate Dynam.*, **36**, 2037-2049. <https://doi.org/10.1007/s00382-011-1058-5>.
- Chae, D.E., Kim, E.J., Kim, J.S. and Lee, S.H. (2020), "Impact of topographic forcing and variation of lower-level jet on local precipitation in southeast region of Korean peninsula", *J. Environ. Sci. Int.*, **29**, 1-13. <https://doi.org/10.5322/JESI.2020.29.1.1>.
- Corral, A.F., Braun, R.A., Cairns, B., Goroooh, V.A., Liu, H., Ma, L. and Sorooshian, A. (2021), "An overview of atmospheric features over the western north atlantic ocean and north american east coast - part I: analysis of aerosols, gases, and wet deposition chemistry", *J. Geophys. Res. Atmos.*, **126**(4), e2020JD032592. <https://doi.org/10.1029/2020JD032592>.
- Cui, C., Zhang, R.H., Wei, Y. and Wang, H. (2021), "Mesoscale wind stress-SST coupling induced feedback to the ocean in the western coast of South America", *J. Oceanol. Limnol.*, **39**, 785-799. <https://doi.org/10.1007/s00343-020-0182-7>.
- Dee, D.P., Uppala, S.M., Simmons, A.J., Berrisford, P., Poli, P., Kobayashi, S. and Vitart, F. (2011), "The era-interim reanalysis: configuration and performance of the data assimilation system", *Quarterly J. Royal Meteorol. Soc.*, **137**(656), 553-597. <https://doi.org/10.1002/qj.828>.
- Dennis, E.J. and Kumjian, M.R. (2017), "The Impact of vertical wind shear on hail growth in simulated supercells", *Amer. Meteorol. Soc.*, **74**, 641-663. <https://doi.org/10.1175/JAS-D-16-0066.1>.
- Fan, L., Shin, S.I., Liu, Z. and Liu, Q. (2016), "Sensitivity of asian summer monsoon precipitation to tropical sea surface temperature anomalies", *Climate Dynam.*, **47**(7), 2501-2514.
- Golding, W.L. (2005), "Low-level wind shear and its impact on airlines", *J. Aviat. Aerosp. Edu. Res.*, **14**(2), 35-45. <https://doi.org/10.1007/s00382-016-2978-x>.
- Huang, T., Yang, Y., O'Connor, E.J., Lolli S., Haywood J., Osborne, M., Cheng, J.C.H., Guo J. and Yim S.H.L. (2021), "Influence of a weak typhoon on the vertical distribution of air pollution in Hong Kong: A perspective from a Doppler LiDAR network", *Environ. Pollut.*, **276**, 116534. <https://doi.org/10.1016/j.envpol.2021.116534>.
- Hunter, R., Pedersen, T.F., Dunbabin, P., Antoniou, A., Frandsen, S., Klug, H., Albers, A. and Lee, W.K. (2001), "European wind turbines testing procedure developments. Task 1: Measurement method to verify wind turbine performance characteristics", *Riso National Laboratory, RISOE R-1209 (EN)*.
- Ji, H.E., Lee, S.H., Park, C. and Lee, H.W. (2014), "A case study on sea breeze circulation and ozone concentration due to the effect of cold water in the southeastern coastal area of Korea", *J. Environ. Sci. Int.*, **23**(2), 261-274. <https://doi.org/10.5322/JESI.2014.23.2.261>.
- Kim, D.Y., Kim, Y.H. and Kim, B.S. (2021a), "Changes in wind turbine power characteristics and annual energy production due to atmospheric stability, turbulence intensity, and wind shear", *Energy*, **214**, 119051. <https://doi.org/10.1016/j.energy.2020.119051>.
- Kim, H., Moon, C.J., Kim, Y.G., Chon, K.H., Joo, J.Y. and Ryu, G.H. (2021), "Analysis of atmospheric stability for the prevention of coastal disasters and the development of efficient coastal renewable energy", *J. Coastal Res.*, **114**, 241-245. <https://doi.org/10.2112/JCR-SI114-049.1>.
- Klotz, B.W. and Jiang, Haiyan (2017), "Examination of surface wind asymmetries in tropical cyclones. Part 1: General structure and wind shear impacts", *Amer. Meteorol. Soc.*, **145**(10), 3989-4009. <https://doi.org/10.1175/MWR-D-17-0019.1>.
- Liu, W.T., Xie, X. and Niler P.P. (2007), "Ocean-Atmosphere interaction over agulhas extension meanders", *J. Climate*, **20**(23), 5784-5797. <https://doi.org/10.1175/2007JCLI1732.1>.
- Lu, Z., Stefano, L. and Giacomo, V.L. (2020), "Lidar measurement for an onshore wind farm: wake variability for different incoming wind speeds and atmospheric stability regimes", *Wind Energy*, **23**(3), 501-527. <https://doi.org/10.1002/we.2430>.
- Pedersen, M.M., Larsen, T.J., Madsen, H.A. and Larsen, G.C. (2019), "More accurate aeroelastic wind-turbine load simulations using detailed inflow information", *Wind Energy Sci.*, **4**(2), 303-323. <https://doi.org/10.5194/wes-4-303-2019>.
- Piotr, S., Anita, B., Jakub, B., Bogdan, B., Lukasz, C., Michal, G. and Miroslav, Z. (2021), "Measurement report: effect of wind shear on PM10 concentration vertical structure in the urban boundary layer in a complex terrain", *Atmos. Chem. Phys.*, **21**, 12113-12139. <https://doi.org/10.5194/acp-21-12113-2021>.
- Qu, B., Gabric, A.J., Zhu, J.N., Lin, D.R., Qian, F. and Zhao, M. (2012), "Correlation between sea surface temperature and wind speed in greenland sea and their relationships with NAO variability", *Water Sci. Eng.*, **5**(3), 304-315. <https://doi.org/10.3882/j.issn.1674-2370.2012.03.006>.
- Ryu, G.H., Kim, D.H., Lee, H.W., Park, S.Y. and Kim, H.G. (2016), "A study of energy production change according to atmospheric stability and equivalent wind speed in the offshore wind farm using CFD program", *J. Environ. Sci. Int.*, **25**(2), 247-257. <https://doi.org/10.5322/JESI.2016.25.2.247>.
- Ryu, G.H., Kim, H., Kim, Y.G., Chon, K.H., Joo, J.Y. and Moon, C.J. (2021), "GIS-based site analysis of and optimal offshore wind farm for minimizing coastal disasters", *J. Coastal Res.*, **114**, 246-250. <https://doi.org/10.2112/JCR-SI114-050.1>.
- Ryu, G.H., Kim, Y.G., Kwak, S.J., Choi, M.S., Jeong, M.S. and Moon, C.J. (2022), "Atmospheric stability effects on offshore and coastal wind resource characteristics in South Korea for developing offshore wind farms", *Energies*, **15**(4), 1305. <https://doi.org/10.3390/en15041305>.
- Ryu, G.H., Kim, D., Kim, D.Y., Kim, Y.G., Kwak, S.J., Choi, M.S. and Moon, C.J. (2022), "Analysis of vertical wind shear effects on offshore wind energy prediction accuracy applying rotor equivalent wind speed and the relationship with atmospheric stability", *Appl. Sci.*, **12**(14), 6949. <https://doi.org/10.3390/app12146949>.
- Seroka, G., Fredj, E., Kohut, J., Dunk, R., Miles, T. and Glenn S. (2018), "Sea breeze sensitivity to coastal upwelling and synoptic flow using lagrangian methods", *J. Geophys. Res. Atmos.*, **123**(17), 9443-9461. <https://doi.org/10.1029/2018JD028940>.
- Xin-Yong, S., Tao1, Q., Wen-Yan, H. and Xiao-Fan, L. (2013), "Effects of vertical wind shear on the pre-summer heavy rainfall budget: A cloud-resolving modeling study", *Atmos. Ocean. Sci. Letters*, **6**(1), 44-51. <https://doi.org/10.1080/16742834.2013.11447048>.
- Wagner R., Antoniou I., Pedersen S.M., Courtney M.S. and Jorgensen, H.E. (2009), "The influence of the wind speed profile on wind turbine performance measurements", *Wind Energy*, **12**(4), 348-362. <https://doi.org/10.1002/we.297>.
- Wharton S. and Lundquist J.K. (2012), "Atmospheric stability affects wind turbine power collection", *Environ. Res. Letters*, **7**(1), 1-9.

- Wen, B., Sha, W., Kexiang, W., Wenxian, Y., Zhike, P. and Fulei, C. (2017), "Power fluctuation and power loss of wind turbines due to wind shear and tower shadow", *Frontiers, Mech. Eng.*, **12**(3), 321-332. <https://doi.org/10.1007/s11465-017-0434-1>.
- Yoo, J.W., Lee, S.H. and Lee, H.W. (2014), "Numerical study on the characteristics of TKE in coastal area for offshore wind power", *J. Environ. Sci. Int.*, **23**(9), 1551-1562. <https://doi.org/10.5322/JESI.2014.23.9.1551>.

CC